Flow kinetic energy conversion from vibration of cylinder arrays due to fluidelastic instability.

B. de Pedro Palomar [(1)], J. Parrondo Gayo [(2)], J. Fernández Oro [(3)]

E.P.I de Gijón, Departamento de Energía, Área de Mecánica de Fluidos.
[(1)] Tlf: 985182661, email:badpdro@hotmail.com
[(2)] parrondo@uniovi.es [(3)] jesusfo@uniovi.es

1. Introduction – This research deals with the fluid-dynamic excitation of vibrations of cylinder arrays subjected to cross-flow due to the mechanism known as Fluidelastic Instability (FI). In this phenomenon, the cross-flow and the cylinders become a dynamically unstable system, i. e., with negative net–damping, when the velocity of the cross-flow exceeds a certain critical value [1]. F I has been responsible for self-excited vibrations with large amplitude in industrial equipment such as shell-and–tube heat exchangers. Because of its potential for the damage of the tubes, the phenomenon has been extensively investigated in the past in order to obtain correlations that can be used to predict critical velocity of the cross-flow at the design stage. However, the complexity of the flow-structure interactions involved produces a considerable uncertainly in those correlations so that large security coefficients have to be used to avoid F I in practise [1, 2].

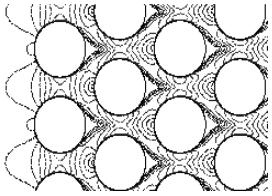

Fig 1: Velocity fields of a normal triangular array.

Nevertheless, the F.I. phenomena also arises the possibility for a controlled extraction of kinetic energy from fluid streams, by conversion to mechanical energy in the vibrating cylinders and subsequent conversion to electrical energy. This is the purpose of the current investigation undertaken by the authors. It represents a novel application in line with some other recent studies on the flow-induced vibrations of cylindrical structures by vortex-shedding mechanisms as a renewable energy technology [3].

2. Methodology – In order to explore the energy capability for conversion associated to the FI phenomena, this paper proposes a methodology based on the CFD simulation of the unsteady flow through arrays of cylinders at velocities above critical. This implies that the non-linear terms of the fluid-structure system become dominant. The purposes of this research require that the vibrating motion of the cylinders is included in the CFD simulations as unsteady boundary conditions [4].

Simulation tests have been conducted on a number of configurations with different geometry and physical characteristics. In each case, one or more cylinders could be allowed to vibrate according to some prescribed pattern. Each simulation produces the time evolution of the velocity (Fig. I) and the pressure fields, as well as the fluctuating lift and drag forces imposed on the cylinders which are analysed in time (Figs. II) and frequency (Fig. III) basis. Afterwards the resulting fluid-dynamic forces can be incorporated in the equation of motion of the cylinder in order to study their structural response. In particular, critical conditions for instability can be established.

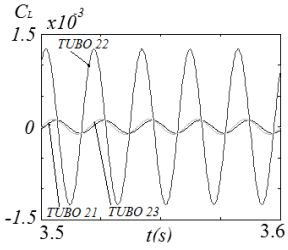

Fig II: Lift coefficients in a row when one of the tubes is vibrating..

2.1. Fluid Dynamics Numerical Model – An in-line square and a normal triangle tube arrays similar to those investigated in [4] and a parallel triangle tube array reproducing the geometry studied in [5] are considered in this work. The CFD model solves the unsteady turbulent flow and provides frequency domain forces that are used to calculate the F.I. threshold. Resulting points can be then compared with the instability predictions for each geometry type obtained in previous theoretical and experimental studies [1, 4, 5]. Good agreement with published data in the scientific literature would allow the validation of this numerical methodology, justifying its application for the proposed analysis of energy extraction viability.

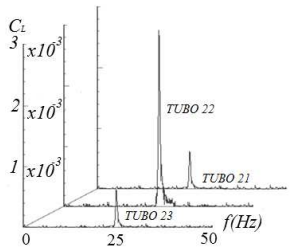

Fig III: FFT in a row when one of the tubes is vibrating..

Simulations were carried out using the ANSYS-FLUENT commercial software. This program allows dynamic domains during calculation, i.e., with varying boundaries over time and adaptive remeshing at each time step. This property permitted to reproduce the vibration of the tubes using UDF programming.

Figs. IV, V and VI show a schematic of the tube geometries for the in-line

Fig IV: Schematic of the normal triangular tube array geometry.

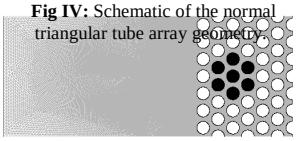

Fig V: Schematic of the normal triangular tube array geometry.

square array, the normal triangle array and the parallel triangle array analysed respectively. The square array (Fig. IV) consists of 49 tubes arranged in seven rows and seven columns. The tube diameter d is 30mm and the pitch to diameter ratio p/d=1.33. The normal triangle tube array (Fig. V) contains 52 tubes arranged in seven columns and nine rows, with d=30mm and p/d=1.35. Finally, the parallel triangle array (Fig. VI) is composed by 18 tubes arranged in six columns and six rows, with d=10mm and p/d=1.57.

Previous sensibility tests were performed in order to select adequate calculation parameters regarding mesh characteristics (such us cells geometry, nodes distribution around de moving tubes or mesh resolution), simulation domains, boundary conditions, turbulence models or time step sizes. Meshes with 147191, 177621 and 15390, nodes were used in the studies for in-line square, normal triangle and parallel triangle arrays, respectively. Triangular cells were selected to avoid the mesh degradation observed in quadrilateral cell simulation tests. The selected mesh distribution around the moving tube is shown in Fig. VII. A time step $\Delta t=T/100$ (T = oscillation period) was found to be appropriate to ensure accurate calculations with an efficient use of computational resources, which is in agreement with other authors suggestions [4]. To reduce boundary layer effects, sidewalls were simulated as symmetry surfaces and tubes of the first and last rows were considered embedded in these surfaces (Figs IV, V and VI). The K-ω Shear Stress Transport (SST) model was used for turbulence closure because of its suitability to account for the effects of flow mixing in the wake of the tubes [4].

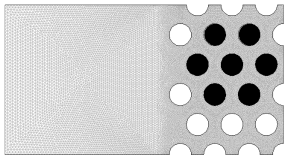

Fig VI: Schematic of the parallel triangular tube array geometry.

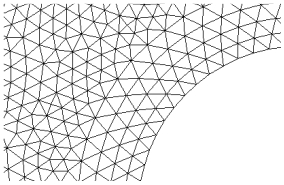

Fig VII: Mesh distribution around the moving tube.

A uniform inlet velocity was applied with a turbulence intensity level of 3%. The gaps between the tubes in the last row were set as constant pressure outlet. In all cases one of the tubes was forced to oscillate in the lift direction with a prescribed excitation frequency, in order to obtain a required reduced flow velocity. The simulation was initiated with an unsteady flow executed with all the tubes being static. Once convergence for the static case was met, the tubes were set into motion and computations were performed with dynamic meshes. Periodic results could be obtained after 20-30 oscillations set off from the static initial solution.

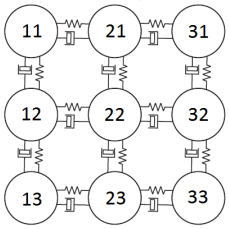

Fig VIII: In-line square array tube motion model.

2.2. Flow-tubes coupled model – The governing equations for a tube motion subjected to forces in both flow direction (x) and transversal direction (y) can be expressed by:

$$m\ddot{x} + c\dot{x} + kx = F_x \qquad (Eq.\ 1)$$

$$m\ddot{y} + c\dot{y} + ky = F_y \qquad (Eq.\ 2)$$

where m, c and k are the tube's structural inertia, damping and stiffness properties. F_x and F_y are drag and lift forces (motion dependent i.e., unsteady) experimented by the tube. The unsteady flow forces acting on the *i-th* tube (lift F_{xi} and drag F_{yi}) can be expressed as the sum of all forces due to its own motion and those of the neighbouring tubes [4].

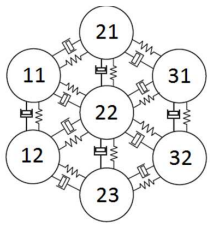

Fig IX: Normal triangle array tube motion model.

The estimation of the critical flow velocity involves identifying the dynamic instability threshold conditions, namely the flow velocity value at which the net damping vanishes.

For the in-line square tube array a system of nine flexible tubes surrounded by fixed tubes was considered (Fig. VIII). For this study only one tube (the central one, denoted as 22) was forced to vibrate at a fixed frequency introduced in the UDF code, so that the source for flow disturbances could be isolated. The unsteady lift and drag forces acting on tubes 11-33 were obtained by integrating the pressure and viscous stresses acting on each tube's surface. A system comprised of seven flexible tubes (11-32) was used for the simulations of the normal triangle array (Fig. IX). As in the previous case only tube 22 was forced to vibrate. Finally, Fig. X shows the system considered for the normal triangle array, where TF is the vibrating tube and tubes T1-T4 are the surfaces where pressure fluctuations were analysed.

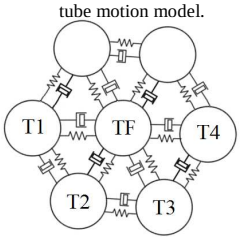

Fig X: Parallel triangle array tube motion model.

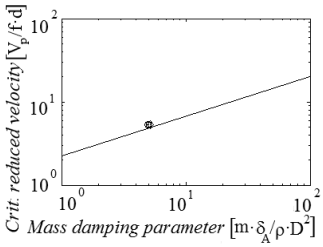

Fig XI: Stability map for in-line square array [1].

3. Results — The results presented in this section are based on the unsteady flow simulations conducted for a range of reduced velocities going from 6 to 13 using the configurations shown in Figs. IV, V and VI. A complete unsteady simulation gave the tube forces along time (Fig II), which, following a FFT analysis of the data (Fig. III), provided force coefficient amplitudes and associated phase. The lift and drag force amplitudes and phase angles were obtained and used to calculate stability threshold data for each array geometry.

3.1. Stability threshold predictions – To validate the results of the calculation procedure now proposed, the predictions have been compared to the design guidelines provided by Weaver and Fitzpatrick [1].

These authors collected the most reliable experimental data available at that time and plotted the stability lines that ensured safe operation without FI as shown in Fig. XI, XII and XIII, regardless the *p/d* parameter. These figures also present the critical threshold data obtained in this study.

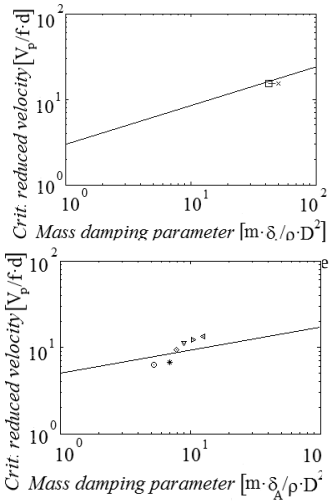

Fig XIII: Stability map for parallel triangle array [1].

A good agreement is observed for the cases of the in-line square and the normal triangle array. Most of the data, however, corresponds to the parallel triangular array, and for this case a somewhat higher deviation is observed, especially for the higher values of the mass-damping parameter. This can be partly attributed to the large value of the *p/d* parameter. Nevertheless, the trend of the data is similar to the Weaver-Fitzpatrick's line and, on the other hand, the experimental data they had used was particularly sparse for the case of the parallel triangular array. In conclusion, the predictions of the model can be considered adequate enough for the purposes of this on-going research, which is the study of the fluid-structure system under FI.

3.2. Propagation pattern for pressure fluctuations – The critical conditions for instability are very much dependent on the way these perturbations are transmitted along de cross-flow and, in particular, on the delay of the flow following the oscillations of the tubes. To further asses on the accuracy of the numerical methodology, experimental study on pressure waves propagation in the parallel triangle array [5] was reproduced.

For the study of pressure waves propagation, in [5] a tube array with the parallel triangular geometry reproduced in Fig. VI was nested in a water tunnel. Only one tube of the array (TF) was flexible enough to vibrate under the range of flow rates used, so that the source of flow disturbances could be isolated. For stepped increments of the cross-flow velocity, two signals were simultaneously captured and analysed: the tube acceleration signal and the fluctuating pressure signal at the surface of four of the fixed tubes placed at a given position along the cross flow, both up and down stream of the vibrating tube (T1-T4). This permitted that the pressure fluctuations data, regarding both amplitude and phase could be correlated with the vibration of the flexible tube. Results of this experimental study are represented in Figs. XIV(a) and XV(a). The values obtained were finally compared to the predictions of the Lever and Weaver's theory (Fig. XIII).

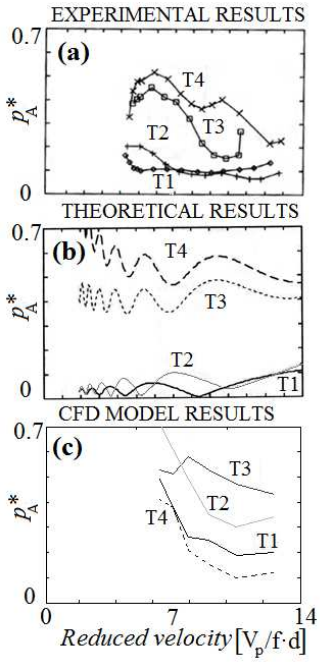

Fig XIV: Pressure amplitude curves.

In their theoretical study Weaver and Lever modelled the fluid mechanics using the unsteady Bernoulli equation with a phase lag, based on a hydraulic transient analogy, to account for the effect of the inertia [6]. From this model, in [5] it was developed a numerical solver algorithm that obtained the amplitude and phase lag introducing the cross flow velocity value. Figs. XIV(b) and XV(b) show the pressures amplitude and phase lag curves for the reduced velocity values considered in the experimental study, being the dimensionless pressure P_A* defined as follows:

$$P_A^* = \frac{P_A}{\rho \cdot U_0 \cdot y_0 \cdot 2\pi f} \quad (Eq.\ 3)$$

where P_A represents the pressure waves amplitude, y_0 is the tube's oscillation amplitude and f is the vibration frequency.

In the present study numerical simulations of the cross flow through the parallel triangle array (Fig. VI) were undertaken, for the same reduced velocity ranges considered in [5].

Fig. XIV(c) and Fig. XV(c) show, respectively, the amplitude and phase lag obtained with the numerical model. Although the reduced velocity range is not large enough to extract clear conclusions about the variable trends, both pressure amplitude and phase lag results seem to be good in quantitative accordance.

Concerning the pressure amplitude curves (Fig. XIV), good agreement between the three studies is observed in T2 and T3 curves. Major differences were observed in T1 and T4 simulation results. Unlike the previous studies, T4 was found to be lower than the other tubes' amplitudes, while T1 values were higher than expected according with the previous works, this divergence in the simulation results is probably due to the low cross-flow rate at which simulations were conducted.

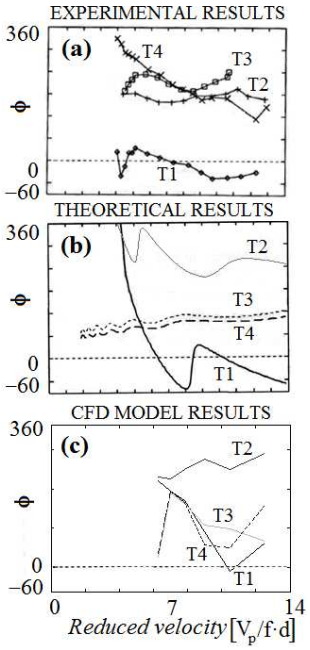

Fig XV: Phase lag curves.

In reference to the phase lag results (Fig. XV), curves obtained with the present CFD model show a good qualitative and quantitative agreement with theoretical model for reduced velocities higher than 7. However, for lower values of this variable, results of the present model invert their trends and seem to agree better with those reported by the experimental work [5].

4. Conclusions – Numerical simulation of cross flow through three tube arrays with different geometries were undertaken. Pressure and force values obtained in the simulations were employed to obtain instability conditions of the flow-tubes coupled system, as well as transmission patterns for the pressure waves in the flow. The predicted critical velocity and pressure wave's behaviour were found to be in good agreement with theoretical and experimental data shown in other previous studies from other authors [1, 4, 5]. The good agreement found confirms the adequacy of the CFD methodology proposed here, and devises the possibility for controlled FI vibrations to be used as a feasible technology to extract energy from a fluid stream.

5. Acknowledgements – This research is included in the activities of the project SACIP (references PC10-69-C1/2) that is funded by "Plan de Ciencia, Tecnología e Innovación (PCTI) de Asturias 2006-2009" and the "Programa Operativo Feder del Principado de Asturias 2007-2013".

6. References –

[1] D.S. Weaver, J. A. Fitzpatrick. "A review of cross-flow induced vibrations in heat exchanger tube arrays" 1988. J. Fluids and Structures, 2, 73-93.

[2] Parrondo J.L., D.S. Weaver, C. Santolaria. "Fluidelastic instability in a tube array subjected to partial admission water cross-flow" 1997. J. Fluids and Structures. 11, 159-181.

[3] M. Bernitsas, K. Raghavan, Y. Ben-Simon. "VIVACE (vortex induced vibration aquatic clean energy): A new concept in generation of clean and renewable energy from fluid flow" 2008. J. of Offshore Mechanics and Arctic Engineering 130(4), 041101.

[4] Hassan M, Gerber A, Omar H. 2010. "Numerical Estimation of Fluidelastic Instability in Tube Arrays". J.Pressure Vessel Technol. 132 (4), 041307.

[5] J. L. Parrondo Gayo. J. Delgado Matarranz. J. Fernández Francos, J. Gonzalez Pérez. "Dynamic presure fields in heat exchanger cross flow subjected to fluidelastic instabilitiy conditions: Theoretical predictions and experimental results" 1997. Revista Iberoamericana de Ingenería Mecánica 57-68.

[6] J. H. Lever and D.S. Weaver "A theoretical model for fluid elastic instability in heat exchanger tube bundles" 1982. Journal of Pressure Vessel Technology 104, 147-158.